# Maximum Torque per Ampere Control of Brushless Doubly Fed Induction Generator Using Variable Structure Approach for Wind Turbine Applications

Hamid Reza Mosaddegh and Hossein Abootorabi Zarchi

**Abstract.** In this paper, a variable structure controller is proposed to control the torque of brushless doubly fed induction generator with considering maximum torque per Ampere (MTPA) strategy. Based on this control approach, a sliding mode controller with a PI is designed in order to reduce the torque pulsations during steady-state behavior while the fast response and robustness merits of the classic DTC are preserved. Also this method decreases the copper losses with minimizing the magnitude of power and control windings currents without deteriorating the dynamic performance. The presented method, guarantees maximum power point tracking (MPPT) with a desirable operation. The simulation results verify an accurate, quick and robust operation of the brushless doubly fed induction generator for wind turbine applications.

**Keywords:** Brushless doubly fed induction generator (BDFIG), Maximum Torque Per Ampere (MTPA), Sliding mode control (SMC), Torque control, Wind turbine.

## 1. Introduction

Brushless doubly fed induction generator (BDFIG) is a single frame and brushless machine which has two 3-phase windings that are set on the stator. One of them is power winding (PW) that is directly connected to the grid. Most of power is exchanged between the BDFIG and grid through this winding. The other winding connected to the grid through a back-to-back converter with less capacity than the generator, is called control winding (CW) [1]. The converter at generator side has the duty of speed control and controlling the reactive power of generator but the converter at grid side, controls the voltage of DC link and regulates the terminal voltage by absorbing or supplying reactive power [2]. It must be mentioned that the control winding capacity is dependent on the desired speed range and reactive power requirements [3].

Because of some advantages like elimination of brushes (high reliability and low maintenance) and the use of a fractionally-rated frequency converter, BDFIG have been paid attention to use in some industrial operations like wind – power generation [1].

The special rotor structure of this generator increases the complexity and produces undesirable spatial harmonics which decrease machine efficiency [4].

Due to limitations of efficiency improvement through the machine design, in recent years, several publications have been released in the field of ac machine drives optimization techniques [5]-[7], but few papers have been reported regarding access to maximum efficiency for BDFIG.

For high performance drives, it is desirable to achieve optimum operation at MTPA. MTPA strategy is a smart answer to the call for efficiency. In principle, the target of MTPA strategy is to deliver the electromagnetic torque with the lowest current magnitude. In this way, copper losses are minimized and the overall system efficiency is increased, at least as long as copper losses are dominant [8]. It should be mentioned that the core losses in a BDFIG are not offered yet, so it is impossible to formulate all loss components and analyzed them, numerically [9]. Therefore, in this paper, core losses are neglected while the stator currents are minimized under the constraint of constant torque at a certain speed.

In this research, a nonlinear controller is introduced on the basis of Linear and Variable Structure Control (LVSC), to drive the BDFIG in wind turbine systems, considering the MTPA control strategy. The proposed method improves the operation of control system by capturing the maximum torque from wind and hence increases the efficiency of wind turbine. Also, without deteriorating the dynamic performance, the presented MTPA approach decreases the copper losses with minimizing the magnitude of power and control winding currents.

## 2. Introduction to BDFIG

### *A. BDFIG Operation*

The stator of this generator has two windings which have different numbers of pole pairs to prevent direct coupling between them. Also, in order to reduce the electromagnetic forces on the rotor, the difference between pole pairs must be greater than one [10]

$$\left|p_1 - p_2\right| > 1, \tag{1}$$

where $p_1$ and $p_2$ are PW and CW pole pairs, respectively.

The rotor of this generator is designed with a special manner. The most conventional structure used in the rotor of this generator is nested-loop. The number of nests which is the number of rotor poles is equal to the sum of PW and CW pole pairs so as to cause indirect coupling between CW and PW [2].

Manuscript received January 14, 2014; revised November 23, 2014; accepted February 5, 2015.
The authors are with the Department of Electrical Engineering, Ferdowsi University of Mashhad, Iran.
The corresponding author's e-mail is: hzarchi@gmail.com.

Owing to special structure of rotor, there will be different modes of operation for this machine. But the best operation of BDFIG is achieved in synchronous mode. In this mode, the frequency of induced voltage in PW, due to indirect coupling with CW, is equal to grid frequency. This situation leads to generation of two fields that turn at the rotor speed. Also, according to the number of rotor poles, in order to establish the indirect coupling between PW and CW, that is fundamental of torque generation in this machine, the direction of rotation of PW magneto-motive force (mmf) respect to the rotor, will be in opposite direction of CW mmf. In this condition [10]

$$\omega_1 - p_1\omega_r = -(\omega_2 - p_2\omega_r) \tag{2}$$

So, the synchronous rotor speed is determined as follow:

$$\omega_r = \frac{\omega_1 + \omega_2}{p_1 + p_2} \tag{3}$$

where $\omega_1$ and $\omega_2$ are PW and CW angular speed, respectively.

If the CW current is dc, the natural speed will be achieved as [11]

$$\omega_n = \frac{\omega_1}{p_1 + p_2} \tag{4}$$

The slips for the two windings are defined as [11]

$$s_1 \triangleq \frac{\frac{\omega_1}{p_1} - \omega_r}{\frac{\omega_1}{p_1}} = \frac{\omega_1 - p_1\omega_r}{\omega_1} \tag{5}$$

$$s_2 \triangleq \frac{\frac{\omega_2}{p_2} - \omega_r}{\frac{\omega_2}{p_2}} = \frac{\omega_2 - p_2\omega_r}{\omega_2} \tag{6}$$

where $s_1$ and $s_2$ are PW and CW slips, respectively.

The BDFIG can be modeled as two induction generators in a common frame. The equivalent circuit of machine is depicted in Fig. 1. The parameters of mentioned circuit are referred to PW side and the power losses are neglected. This circuit is valid for all operation modes of BDFIG including synchronous mode [12].

*B. BDFIG Model*

The generator model in PW flux frame is expressed by the following [1]

$$V_1 = R_1 I_1 + \frac{d\psi_1}{dt} + j\omega_1\psi_1 \tag{7}$$

$$\psi_1 = L_1 I_1 + L_{1r} I'_r \tag{8}$$

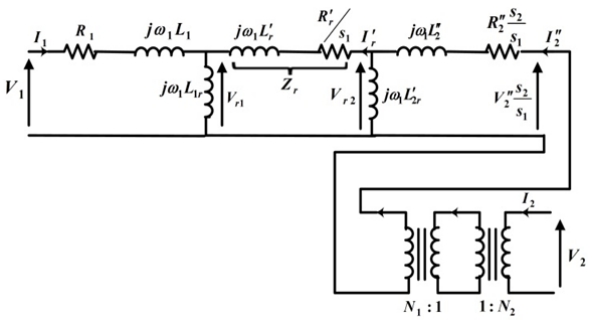

Fig. 1. BDFIG Referred Per-Phase Equivalent Circuit [12].

$$V''_2 = R''_2 I''_2 + \frac{d\psi''_2}{dt} + j(\omega_1 - (p_1 + p_2)\omega_r)\psi''_2 \tag{9}$$

$$\psi''_2 = L''_2 I''_2 + L'_{2r} I'_r \tag{10}$$

$$V'_r = R'_r I'_r + \frac{d\psi'_r}{dt} + j(\omega_1 - p_1\omega_r)\psi'_r \tag{11}$$

$$\psi'_r = L'_r I'_r + L_{1r} I_1 + L'_{2r} I''_2 \tag{12}$$

In the above equations, the subscripts *1, 2,* and *r* show PW, CW, and rotor, respectively.

The electromagnetic torque is given by [9]

$$\begin{aligned} T_e = {} & I^2\left[(\frac{n_1}{n_2})^2 L_{2r}^2 p_2 - L_{1r}^2 p_1\right]\frac{R'_r\omega_s}{Z_r^2} \\ & - \frac{n_1}{n_2} I^2 L_{1r}^2 L_{2r}^2 \frac{\omega_s}{Z_r}[(p_2 - p_1)\cos(\psi)\cos(2\delta) \\ & + (p_2 + p_1)\sin(\psi)\sin(2\delta)], \end{aligned} \tag{13}$$

where

$$I_1 = I''_2 = I \Rightarrow I_2 = \left(\frac{n_1}{n_2}\right) I \tag{14}$$

$$\delta = \tan^{-1}\left(\frac{i_{1q}}{i_{1d}}\right) \tag{15}$$

$$\omega_s = p_1\omega_r - \omega_1 \tag{16}$$

$$\psi = \tan^{-1}\left(\frac{\omega_s L'_r}{R'_r}\right) \tag{17}$$

$$Z_r = \sqrt{R'^2_r + (\omega_s L'_r)^2} \tag{18}$$

Also, the mechanical equation of generator is

$$T_L - T_e = B\omega_r + J\frac{d\omega_r}{dt} \tag{19}$$

where $J$ is the moment of inertia, $B$ is the friction coefficient and $T_L$ is the torque produced by wind turbine. The parameters and variables used in (7) – (12) are introduced in Table 1.

Table 1. BDFIG parameters and variables

| | |
|---|---|
| $V, I, \psi, \omega_r$ | Voltage, current, flux vectors and generator speed |
| $R_1, R_2, R_r$ | Resistances of PW, CW and rotor |
| $L_1, L_2, L_r$ | Self-inductances of stator windings and rotor |
| $L_{1r}, L_{2r}$ | Coupling inductances between stator windings and rotor |

## 3. Control Strategy

### *A. MTPA control*

The MTPA strategy is obtained with minimization of CW and PW current magnitude under the constraint of constant torque at a certain speed. Based on Lagrange theorem, it can be easily found that any control strategy can be realized when the torque and its corresponding objective function are tangent at a point or in other words their gradient vectors are in parallel. In MTPA, the minimization of stator current is selected as objective function.

The square PW current of BDFIG can be calculated as

$$I_1^2 = I_{1d}^2 + I_{1q}^2. \tag{20}$$

In this section, the minimization of (20) under the constraint of constant torque is selected as objective function. In Fig. 2, according to (13), the constant torque curve can be drawn as a hyperbola on the $I_{1d} - I_{1q}$ plane. On the same plane, at a speed and with neglecting the iron losses, the curve that representing the square PW current, takes the form of a circle. Under the constraint of constant torque, if an operating point is set at point ‘‘a” in Fig. 2, the curve A is supposed to be a control objective curve such as constant stator current curve ($I_{1a}^2$). If an operating point is set at ‘‘b”, the curve B is another control objective curve ($I_{1b}^2$). Using Lagrange’s Theorem, it can be easily found that control objective is minimum when the torque curve and control objective curve are tangent at a point if and only if their gradient vectors are in parallel. This means that $\nabla T_e(I_{1d}, I_{1q})$ must be a scalar multiple of $\nabla I_1^2(I_{1d}, I_{1q})$ at the point of tangency (see ‘‘b” in Fig. 2), so that

$$\left\|\nabla T_e(I_{1d}, I_{1q})\right\| \left\|\nabla I_1^2(I_{1d}, I_{1q})\right\| \sin\theta = 0, \tag{21}$$

where $\theta$ is the angle between $\nabla T_e(I_{1d}, I_{1q})$ and $\nabla I_1^2(I_{1d}, I_{1q})$.

Criterion of MTPA strategy realization is obtained as follows:

$$y_1 = \left\|\nabla T_e(I_{1d}, I_{1q})\right\| \left\|\nabla I_1^2(I_{1d}, I_{1q})\right\| \sin\theta. \tag{22}$$

It is obvious that the control strategy is realized when $y_1$ is kept at zero. The cross-product of gradient vectors is calculated from the following equation

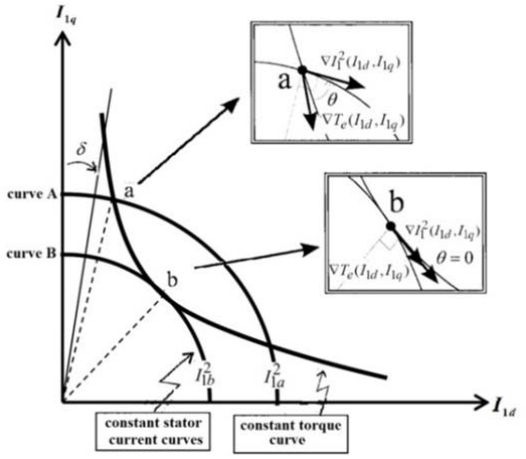


Fig. 2. Constant torque curve and PW current curve on $I_{1d}$ -$I_{1q}$ plane.

$$\nabla T_e(I_{1d}, I_{1q}) \times \nabla I_1^2(I_{1d}, I_{1q}) = \det \begin{bmatrix} i & j & k \\ \dfrac{\partial T_e}{\partial I_{1d}} & \dfrac{\partial T_e}{\partial I_{1q}} & 0 \\ \dfrac{\partial I_1^2}{\partial I_{1d}} & \dfrac{\partial I_1^2}{\partial I_{1q}} & 0 \end{bmatrix} \tag{23}$$

So $y_1$ will be obtained as follows

$$y_1 = \frac{\partial T_e}{\partial I_{1d}} \times \frac{\partial I_1^2}{\partial I_{1q}} - \frac{\partial T_e}{\partial I_{1q}} \times \frac{\partial I_1^2}{\partial I_{1d}} = 0 \tag{24}$$

$$\Rightarrow \frac{I_{1q}}{I_{1d}} = \tan\left(\frac{1}{2}\tan^{-1}\frac{(p_2 + p_1)\sin\psi}{(p_2 - p_1)\cos\psi}\right)$$

With neglecting the core losses, criterion of realization of the MTPA strategy in BDFIG is obtained as (24). Although ideally, the optimum current angle is constant ($\delta \cong 45^\circ$), however, with considering core losses, value of this angle is greater than ideal amount.

### *B. Linear and Variable Structure Control*

Due to nonlinear nature of electrical machines, if the reference voltage is generated by a nonlinear controller, a better operation of electrical drive will be achieved. In this regard, the sliding mode controller because of robustness to uncertainties and variations in system parameters, fast dynamic response and also compensation of disturbance effects, have been paid attention by electrical drive researchers. However, robustness of this controller is only in its sliding phase and the reaching phase is designed so that the mechanical mode paths of system reach to sliding phase as quick as possible. In other words, the dynamic of system is not perfectly robust all the time. So, it is possible that the conventional SMC can not retain its stability against the uncertainties and disturbances. Also the other drawback of this controller is chattering effect, which might be harmful for the system.

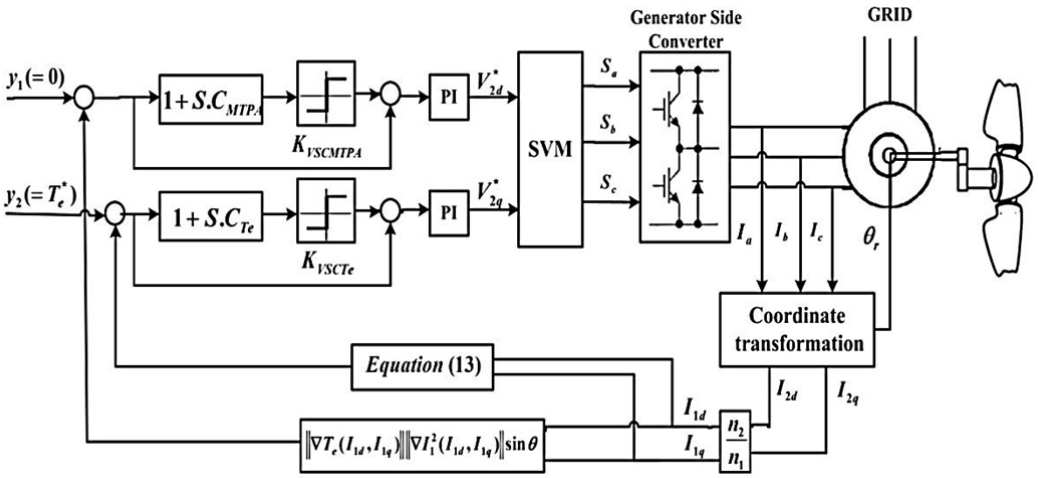


Fig. 3. Block diagram of the proposed BDFIG drive system control

To improve the stability of system against uncertainties and also elimination of chattering in control system, in this paper a control method which is a combination of linear controller (PI) and SMC, introduced as Variable Structure Control (VSC), is proposed. This method, while having the simplicity of implementation, has the greatest features of linear controller (i.e. smooth and without chattering operation) and the feature of SMC (i.e. robustness against uncertainties). Another advantage of this method is independence to system parameters.

The block diagram of Linear and Variable Structure Control (LVSC) that is implemented on generator side converter is shown in Fig. 3. The main task of LVSC is fast and reliable access to control of torque and also achieving the MTPA.

An SVM unit is used to produce switching signals based on voltage references.

The sliding surface is defined as below

$$S_{y_1} = e_{y_1} + c_{y_1}\frac{de_{y_1}}{dt} \tag{25}$$

$$S_{y_2} = e_{y_2} + c_{y_2}\frac{de_{y_2}}{dt} \tag{26}$$

where $e_{y_1} = y_1^* - \hat{y}_1$ is error between the reference $(y_1^* = 0)$ and the cross product of $\nabla T_e(I_{1d}, I_{1q})$ and $\nabla I_1^2(I_{1d}, I_{1q})$. In addition, $e_{y_2} = y_2^* - \hat{y}_2$ is torque error. Superscript "^" shows measured values and "*" shows reference values. Design constants $c_{y_1}$ and $c_{y_2}$ are selected so as to impose the desired dynamics in sliding mode. CW reference voltage, $V_2^* = V_{2d}^* + jV_{2q}^*$ is gained at the output of variable structure controller that $V_{2d}^*$ is obtained by the MTPA control and $V_{2q}^*$ is obtained by torque control law. Sign function, $Sgn(.)$, is used in control law.

$$V_{2d}^* = (K_{Py_1} + \frac{K_{Iy_1}}{s})(e_{y_1} + K_{VSCy_1}\,Sgn(S_{y_1})) \tag{27}$$

$$V_{2q}^* = (K_{Py_2} + \frac{K_{Iy_2}}{s})(e_{y_2} + K_{VSCy_2}\,Sgn(S_{y_2})) \tag{28}$$

In the above equations, $s$ is Laplace operator, $K_{Py_1}$, $K_{Iy_1}$, $K_{Py_2}$, $K_{Iy_2}$ are PI controller gains and $K_{VSCy_1}$, $K_{VSCy_2}$ are variable structure control gains.

With selection of proper coefficients for linear controller and SMC, the best response from the aspect of system robustness and best time response is attainable without chattering effect. It must be considered that in transient condition, linear controller is more dominant and PI coefficients must be set so as to obtain the desired dynamic response. In steady state, SMC is more dominant and the best steady state response can be achieved by optimally setting the $K_{VSCy_1}$ and $K_{VSCy_2}$. It can be proved that large enough values for $K_{VSC}$ fulfill the reaching and stability condition $S.\dot{S} < 0$ [14].

## 4. Wind Turbine and MPPT

### *A. Aerodynamic Model*

The wind turbine extracts the energy of its blades and transmits this energy to the generator. The power absorbed from wind turbine is given below [15]

$$P_{mech} = \frac{1}{2}\pi C_p(\beta,\lambda)\rho R^2 v^3, \tag{29}$$

where $\rho$ is air density, $R$ is turbine radius, $v$ is wind speed and $C_p$ is the turbine power coefficient which its maximum value is 0.59. In a wind turbine, this coefficient

is usually between 0.25 and 0.45. This quantity is depended on tip speed ratio ($\lambda$) and the blade pitch angle ($\beta$). $\lambda$ is obtained by the following equation

$$\lambda = \frac{R\omega}{v}, \tag{30}$$

where $\omega$ is the speed of turbine rotor. In this paper, $\beta$ is supposed to be zero and so $C_p$ is only depended to $\lambda$.

### *B. MPPT Algorithm*

The extracted power from wind turbine is depended on the accuracy of the algorithm of MPPT that ensures maximum energy yielding. The strategies can be classified into two groups [17]: the look-up table based strategies; and the strategies that are independent of aerodynamic characteristics. Some of the control algorithms that require the aerodynamic information are tip speed ratio (TSR) control, power signal feedback (PSF) control and optimum torque (OT) control. The MPPT techniques which do not need aerodynamic characteristics are often known as HCS methods. The two significant control strategies of this category include perturbation and observation (P&O) control and fuzzy logic control (FLC).

In this paper, regarding to BDFIG torque control, the best method to achieve MPPT, is the optimum torque control method. This method is superior to others because of its simplicity and accuracy. The other advantage of this method is that there is no need to have speed controller and wind speed sensor. In this technique the reference value for torque can be obtained using rotor speed and the optimum torque versus generator speed curve. In (31), the optimum torque is expressed as a function of generator speed [16]

$$T_{opt}(\omega) = \frac{0.5\pi\rho\, C_{p\max} R^5}{\lambda^3_{opt}}\omega^2 = K_{opt}\omega^2, \tag{31}$$

With controlling the generator torque in $T_{opt}$, the maximum power can be extracted from wind turbine. $T_{opt}$ is used as the reference torque.

## 5. Simulation Results

In this section, the simulation results are presented to confirm the desirable operation of the proposed control method. Table 2 shows the wind turbine and generator parameters.

The prpoer selection of controllers parameters are important to obtain the desired performance of system. In this paper, the this parameters is selected with trial and error method. The values of PI and SMC parameters are shown in Table 3.

The reference torquesignal is generated by OT MPPT algorithm. As shown in Fig. 5, the generator torque tracks the reference value in variable wind speed pattern correctly. The wind speed profile can be seen in Fig. 4.

The power coefficient of the wind turbine is shown in Fig. 6. One can see that this parameter converges to its maximum value by using the proposed control system. In order to verify the realization of the presented MPPT algorithm, the desirable performance of the control system for tracking $\lambda_{opt}$, has been illustrated in Fig. 7. It tends to capture maximum power from wind turbine and proper implementation of the MPPT algorithm.

Also, with the proposed variable structure control, the MTPA strategy realization is satisfied. The variable $y_1$ always oscillates around its reference value ($y_{1ref} = 0$) that means the strategy has been achieved. The two-axis torque producing currents are shown in Fig. 10 and 11. With strategy realization, q- and d-axis currents will be equal as well, without considering core losses of this machine.

Table 2. Generator and Wind Turbine Parameters

| **Brushless Doubly Fed Induction Generator** | | | |
|---|---|---|---|
| **Parameter** | **Value** | **Parameter** | **Value** |
| PW Pole-Pair | 2 | $L_1$ (mH) | 349.8 |
| CW Pole-Pair | 4 | $L_2$ (mH) | 363.7 |
| Natural speed (rpm) | 500 | $L_{1r}$ (mH) | 3.1 |
| PW rated voltage (V) | 380 | $L_{2r}$ (mH) | 2.2 |
| CW rated voltage (V) | 380 | $L_r$ (mH) | 0.044 |
| Rated torque (N.m) | 50 | $R_1$ (Ω) | 2.3 |
| $J$ (Kg.m$^2$) | 0.53 | $R_2$ ( Ω) | 4.4 |
| $B$ (N.m.s) | 0.036 | $R_r$ ( Ω) | 0.00013 |
| **Wind Turbine** | | | |
| Blade radius (m) | 3.3 | $C_{p\max}$ | 0.436 |
| Gear ratio | 3.2 | Rated wind speed (m/s) | 8 |
| Air density(Kg/m$^3$) | 1.25 | $\lambda_{opt}$ | 8 |

Table 3. The Controller GAINS in Presented Drive System

| **PI parameters** | | **SMC parameters** | |
|---|---|---|---|
| $K_{Py1} = 1.4$ | $K_{Iy1} = .11$ | $c_{y1} = 1$ | $K_{VSCy1} = 250$ |
| $K_{Py2} = 1$ | $K_{Iy2} = .11$ | $c_{y2} = 1$ | $K_{VSCy2} = 250$ |

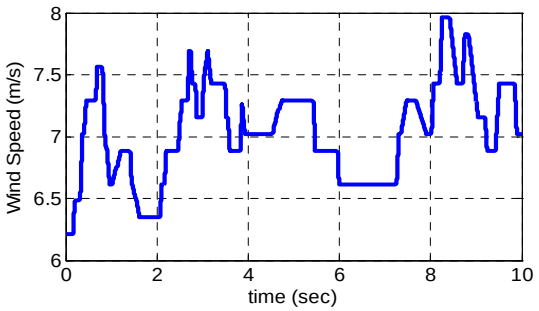


Fig. 4. Wind speed.

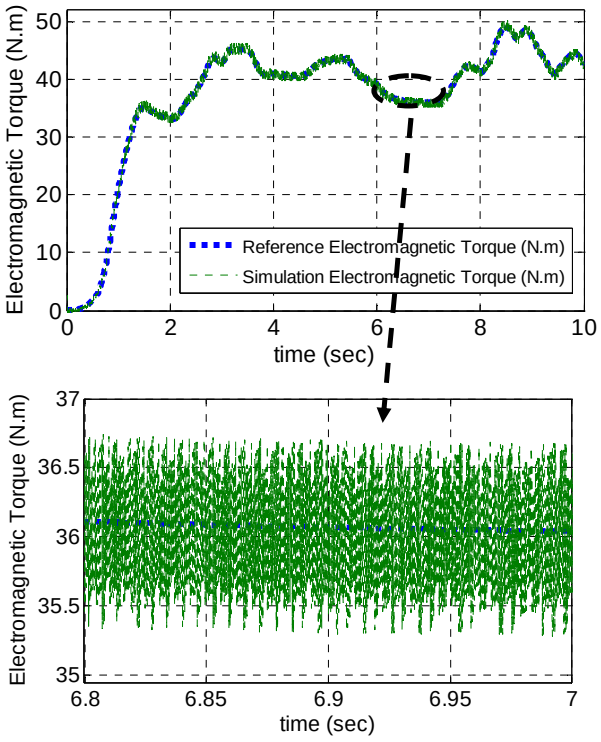


Fig. 5. Generator torque response to wind speed variations.

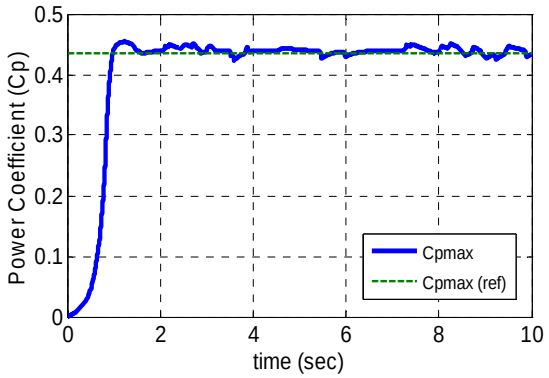


Fig. 6. Power coefficient variation.

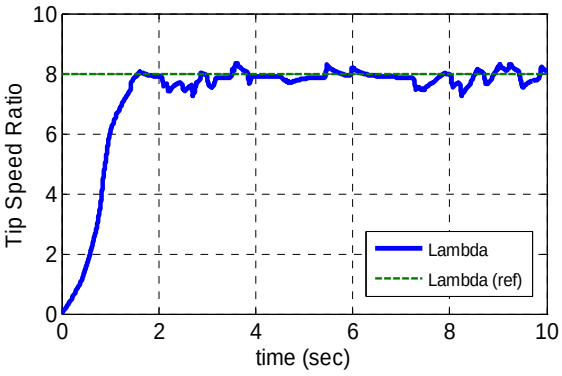


Fig. 7. Maximum power point tracking performance.

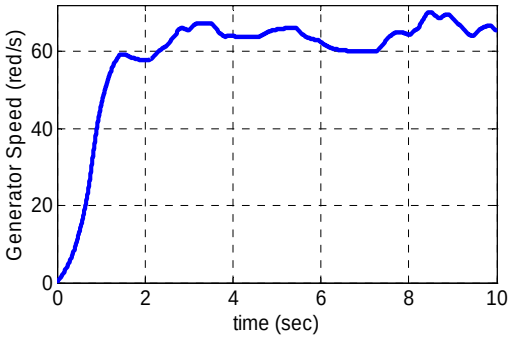


Fig. 8: Generator speed variation

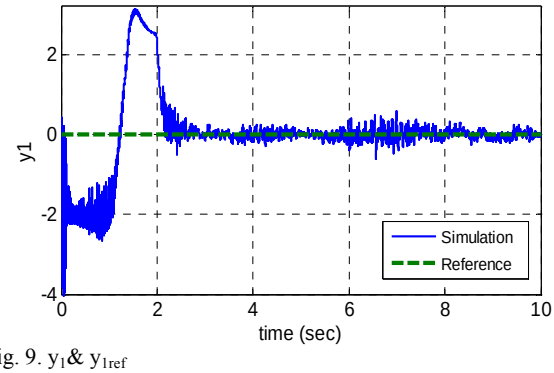


Fig. 9. $y_1$& $y_{1ref}$

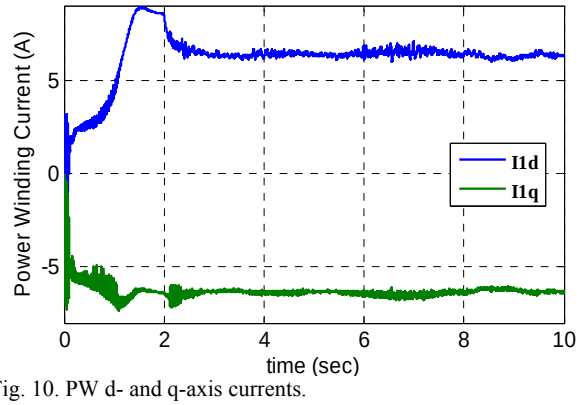


Fig. 10. PW d- and q-axis currents.

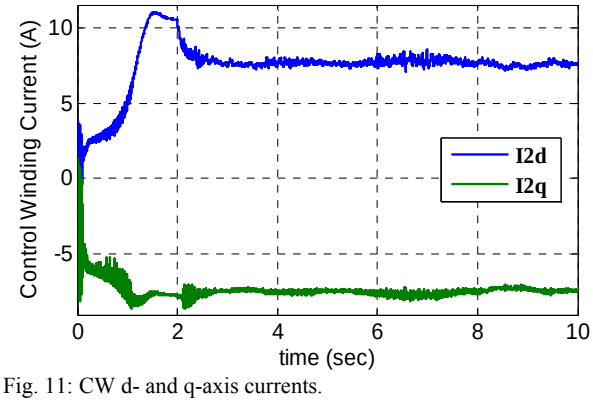


Fig. 11: CW d- and q-axis currents.

## 6. Conclusion

In this paper a variable structure torque control of BDFIG for wind turbine application was proposed and evaluated. The control strategy combines sliding mode controller and PI principles to achieve simple and robust high performance behavior. In particular, SMC makes the drive robust to disturbances and operating point variations, PI controller guaranties a smooth and without chattering operation and SVM improves the steady state responses of torque with reducing the ripple. During transient operation, the proposed approach verified good dynamic response and strong robustness to fluctuations of wind profile. This simple, quick, accurate and robust control strategy guaranties proper performance of MPPT algorithm and therefore best energy capturing from wind turbine. In addition, based on proposed control approach, the MTPA control strategy of BDFIG has been evaluated for wind power applications.

## References


[1] S. Shao, E. Abdi, F. Barati, and R. McMahon, "Stator-flux-oriented vector control for brushless doubly fed induction generator," *IEEE Transactions on Industrial Electronics*, vol. 56, no. 10, pp. 4220-4228, October 2009.

[2] S. Tohidi, M. R. Zolghadri, H. Oraee, P. Tavner, E. Abdi and T. Logan, "Performance of the brushless doubly-fed machine under normal and fault conditions," *IET Electric Power Applications*, vol. 6, Iss. 9, pp. 621–627, 2012.

[3] J. Poza, E. Oyarbide, I. Sarasola, and M. Rodriguez, "Vector control design and experimental evaluation for the brushless doubly fed machine," *IET Electr. Power Appl*., vol. 3, Iss. 4, pp. 247–256, 2009.

[4] H. Gorginpour, H. Oraee, and R. A. McMahon, "Performance description of brushless doubly-fed induction machine in its asynchronous and variable speed synchronous modes," *Journal of Electromagnetic Analysis and Applications*, vol. 3, pp. 490-511, December 2011.

[5] H. D. Lee, S.J. Kang, and S. K. Sul, "Efficiency-optimized direct torque control of synchronous reluctance motor using feedback lineariztion," *IEEE Transactions on Industrial Electronics*, vol. 46, no. 1, pp. 192-198, February 1999.

[6] A. Consoli, G. Scarella, G. Scelba, and A. Testa, "Steady-state and transient operation of IPMSMs under maximum-torque-per-ampere control," *IEEE Transactions on Industry Applications*, vol. 46, no. 1, pp. 121-129, January/February 2010.

[7] M. Hajian, J. Soltani, G. Arab Markadeh and S. Hosseinnia, "Adaptive nonlinear direct torque control of sensorless IM drives with efficincy optimization," *IEEE Transactions on Industrial Electronics*, vol. 57, no. 3, pp. 975-985, March 2010.

[8] S. Bolognami, L. Peretti, and M. Zigliotto, "Oline MTPA control strategy for DTC synchronous-reluctance-motor drives," *IEEE Transactions on Power Electronics*, vol. 26, no. 1, pp. 20-28, January 2011.

[9] M. Ahmadian, B. Jandaghi, and H. Oraee, "Maximum torque per ampere operation of brushless doubly fed machines," *Renewable Energies and Power Quality Journal (RE & PQJ)*, no. 9, pp. 1720-1725, May 2011.

[10] S. WiIliamson, A. C. Ferreira, and A. K. Wallace, "Generalised theory of the brushless doubly-fed machine. Part I: Analysis," *IEE Proc. Electr. Power Appl*., vol. 144, no. 2, pp. 111-122, March 1997.

[11] R.A. McMohan, P.C. Roberts, X. Wang and P.J. Tavner, "Performance of BDFM as generator and motor", *IEE Proceedings - Electric Power Applications*, vol. 153, Iss. 2, pp. 289-299, March 2006.

[12] P. C. Roberts, "A study of brushless doubly-fed (induction) machines," Ph.D. Dissertation, University of Cambridge, 2005.

[13] C. Lascu, I. Boldea, and F. Blaabjerg, "Direct torque control of sensor less induction motor drives: A sliding-mode approach," *IEEE Transactions on Industry Applications*, vol. 40, no. 2, pp. 582-590, April 2004.

[14] O. Anaya-Lara, N. Jenkins, P. Cartwright, and M. Hughes, *Wind Energy Generation: Modeling and Control*. Chichester, West Sussex, United Kingdom: John Wiley and sons, Ltd., pp. 4-6, 2009.

[15] M. Thurston and M. Priestley, "Influence of cracking on thermal response of reinforced concrete bridges," *Concrete International*, vol. 6, pp. 36-43, 1984.

[16] S. M. Kazemi, H. Goto, H. Guo, and O. Ichinokura, "Review and critical analysis of the research papers published till date on maximum power point tracking in wind energy conversion system," *Energy Conversion Congress and Exposition (ECCE)*, pp. 4075-4082, 2010.


**Hamid Reza Mosaddegh** was born in Mashhad, Iran, in 1987. He received the B.Sc. and M.Sc. degrees in electrical engineering from Ferdowsi University of Mashhad (FUM), Mashhad, Iran, in 2011 and 2014, respectively. He is currently working toward the Ph.D. degree at FUM. His research interests are variable-speed ac drives, power electronics and renewable energies.

**Hossein Abootorabi Zarchi** received Ph.D. degree from Isfahan University of Technology, Isfahan, Iran. He was a Visiting Ph.D. Student with the Control and Automation Group, Denmark Technical University, Denmark, from May 2009 to February 2010. He is currently an Assistant Professor in the Faculty of Engineering, Ferdowsi University of Mashhad, Mashhad, Iran. His research interests are renewable energies, electrical machines and applied nonlinear control in electrical drives.